frontiers in Marine Science

ORIGINAL RESEARCH
published: 19 June 2015
doi: 10.3389/fmars.2015.00037

Cold-water coral reefs and adjacent sponge grounds: hotspots of benthic respiration and organic carbon cycling in the deep sea

Cécile Cathalot[1]*, *Dick Van Oevelen*[1], *Tom J. S. Cox*[1,2], *Tina Kutti*[3], *Marc Lavaleye*[4], *Gerard Duineveld*[4] and *Filip J. R. Meysman*[1,5]

[1] Department of Ecosystem Studies, Royal Netherlands Institute for Sea Research, Yerseke, Netherlands, [2] Ecosystem Management Research Group, Universiteit Antwerpen, Wilrijk, Belgium, [3] Department of Benthic Resources and Processes, Institute of Marine Research, Bergen, Norway, [4] Department of Marine Ecology, Royal Netherlands Institute for Sea Research, Den Burg, Netherlands, [5] Laboratory of Analytical, Environmental and Geochemistry, Vrije Universiteit Brussel, Brussels, Belgium

OPEN ACCESS

Edited by:
Hajime Kayanne, The University of Tokyo, Japan

Reviewed by:
Aldo Cróquer, Simon Bolivar University, Venezuela
Toshihiro Miyajima, The University of Tokyo, Japan

***Correspondence:**
Cécile Cathalot, Laboratory of Geochemistry and Metallogeny, Ifremer (Brest), ZI de la Pointe du Diable, CS10070, F-29280 Plouzané, France
cecile.cathalot@ifremer.fr

Specialty section:
This article was submitted to Coral Reef Research, a section of the journal Frontiers in Marine Science

Received: *18 December 2014*
Accepted: *23 May 2015*
Published: *19 June 2015*

Citation:
Cathalot C, Van Oevelen D, Cox TJS, Kutti T, Lavaleye M, Duineveld G and Meysman FJR (2015) Cold-water coral reefs and adjacent sponge grounds: hotspots of benthic respiration and organic carbon cycling in the deep sea. Front. Mar. Sci. 2:37. doi: 10.3389/fmars.2015.00037

Cold-water coral reefs and adjacent sponge grounds are distributed widely in the deep ocean, where only a small fraction of the surface productivity reaches the seafloor as detritus. It remains elusive how these hotspots of biodiversity can thrive in such a food-limited environment, as data on energy flow and organic carbon utilization are critically lacking. Here we report *in situ* community respiration rates for cold-water coral and sponge ecosystems obtained by the non-invasive aquatic Eddy Correlation technique. Oxygen uptake rates over coral reefs and adjacent sponge grounds in the Træna Coral Field (Norway) were 9–20 times higher than those of the surrounding soft sediments. These high respiration rates indicate strong organic matter consumption, and hence suggest a local focusing onto these ecosystems of the downward flux of organic matter that is exported from the surface ocean. Overall, our results show that coral reefs and adjacent sponge grounds are hotspots of carbon processing in the food-limited deep ocean, and that these deep-sea ecosystems play a more prominent role in marine biogeochemical cycles than previously recognized.

Keywords: deep-sea ecosystems, cold-water corals, sponges, respiration, energy flow

Introduction

Cold-water corals and sponges form complex reef structures on the seafloor (**Figure 1**), which support a rich community of suspension-feeding fauna and play a crucial role as a refuge, feeding ground and nursery for various commercial fishes (Miller et al., 2012). These reef ecosystems are widespread across the deep ocean (Klitgaard and Tendal, 2004; Roberts et al., 2006), but they face an uncertain future, as the human imprint on the deep-sea rapidly increases (Pusceddu et al., 2014). As oil and gas exploration are moving into deeper waters, seafloor installations, accidental oil spilling and sediment plumes are increasingly impacting the reef structures (Purser and Thomsen, 2012; Fisher et al., 2014; Roberts and Cairns, 2014), while physical disturbance by intensified bottom trawling significantly damages the slow growing reefs (Fossa et al., 2002; Althaus et al., 2009; Miller et al., 2012).

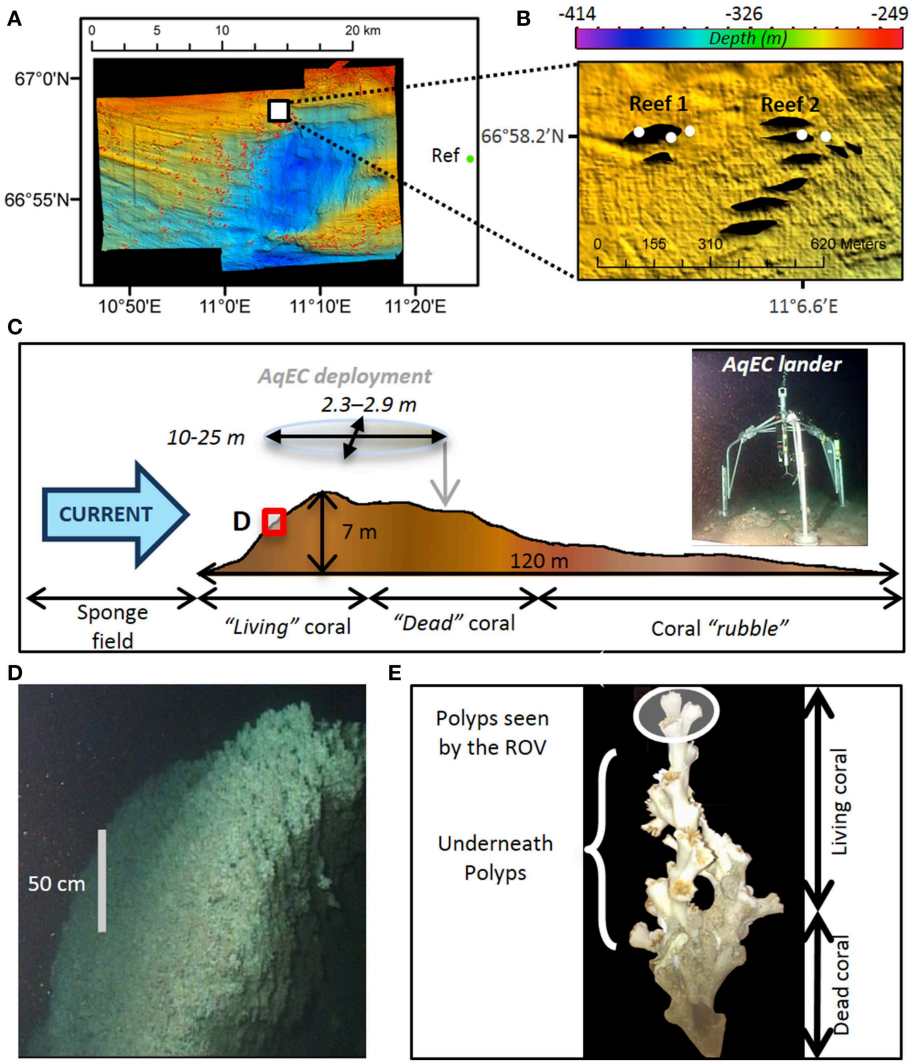

FIGURE 1 | (A) Bathymetry map of the Træna Deep Coral reef field with red dots representing known cold-water coral reef locations. **(B)** Sampling sites: two reefs were investigated and the symbols mark the locations of AqEC deployments. **(C)** Topography of Reef R1. The location of the AqEC deployment is indicated by the gray arrow. The size of the upstream AqEC footprint area, as indicated by the oval shape above the reef, was estimated using the equations in Berg et al. (2007) using the cross correlation among the 3D velocity components to calculate the friction velocity. **(D)** Photograph of a vertical lobe of densely packed branches of living *Lophelia pertusa* at the head of Reef R1. The exact position is indicated by the red square in **(C)**. **(E)** Coral branch sampled by ROV Aglantha. The shaded area indicates the planar view that can be "seen" by the ROV camera. The underlying layers of living and dead polyps remain hidden from the camera's view and are indicated by the accolade.

Cold-water coral ecosystems are also considered to be strongly sensitive to various impacts of climate change. Foremost, ocean acidification is considered a major threat to their future existence, due to the anticipated shoaling of aragonite saturation horizon and the associated reduction in calcification rates (Roberts and Cairns, 2014). Energy availability is considered a prime factor in the sensitivity of cold-water corals to ocean acidification, and therefore, climate-induced shifts in the primary production and export from the surface ocean should also be considered. As rising sea-surface temperatures can reduce water column mixing and intensify the recycling of organic matter in the surface ocean, climate change can decrease the carbon export flux to the deep sea (Bopp et al., 2001). Moreover, the energy demands and respiration rates of the reef-forming species are predicted to increase in a warmer ocean (Dodds et al., 2007; Roberts and Cairns, 2014), thus aggravating the food limitation problem. While the sensitivity to ocean acidification is increasingly addressed in experimental and modeling studies, it is unclear how these climate-induced changes in food supply and respiration will affect the ecosystem functioning of cold-water coral and sponge communities. To resolve this, data on the energy flow and organic carbon (OC) processing rates within these deep-sea ecosystems are critically needed.

A recent food web model analysis from the Logachev Mound complex (NE Atlantic) suggests that OC processing rates in Cold-Water Coral Reefs (CWCR) largely exceed those of the

surrounding soft sediments (Van Oevelen et al., 2009). Moreover, Kutti et al. (2013) estimated that reef-associated sponge grounds can also process considerable amounts of OC, based on sponge abundance data and laboratory-based respiration rates. Yet, until now, there has been no experimental *in situ* validation of this "high OC processing" hypothesis. Community respiration rates in reef environments are difficult to quantify, as the diversity of fauna, habitat complexity and up-scaling issues prevent the use of traditional techniques (e.g., incubation chambers, microsensor profiling). Here we report *in situ* measurements of community respiration rates for CWCR and adjacent sponge grounds, obtained by Aquatic Eddy Correlation (AqEC), which is a novel technique that allows the *in situ* determination of community respiration rates in topographically complex seafloor environments (Berg et al., 2003; Lorrai et al., 2010; Long et al., 2013; Attard et al., 2014). The AqEC technique is non-invasive, and integrates the benthic oxygen flux over a large footprint area ($>10\ m^2$, Berg et al., 2007). Our data show that carbon processing in CWCR and associated sponge grounds is much more intense than previously recognized: these ecosystems not only act as havens of biodiversity, but are true hotspots of organic carbon cycling in a food-limited deep sea.

Materials and Methods

Study Site and Sampling

Data were collected in May 2011 on board R/V Håkon Mosby, on a cruise to the Træna Marine Protected Area (MPA), which covers 300 km^2 of the Norwegian continental margin. The seafloor in the Træna Deep Coral reef field (Norwegian continental shelf) consists of three main habitat types (Buhl-Mortensen et al., 2010; Kutti et al., 2013): (i) elongated, cigar-shaped reefs (100–150 m long, 25–55 m wide and on average 7 m high) formed by the reef-building coral *Lophelia pertusa*, (ii) dense sponge grounds surrounding the coral reefs, consisting of aggregations of large demosponges, and (iii) stretches of bare sediment, containing typical soft-sediment infauna, which are located further away from the reefs and sponge grounds.

We performed three types of data collection (**Table 1**): (i) Aquatic Eddy Correlation (AqEC) lander deployments to obtain *in situ* Community Respiration (CR) rates, (ii) Smøgen box-corer deployments to retrieve soft sediment, living coral branches and dead coral branches for shipboard incubations, and (iii) dives with the Remotely Operated Vehicle (ROV) Aglantha to collect branches of living coral and samples of living sponges, and to obtain video footage for seafloor habitat mapping and estimates of coral and sponge densities. Deployments were done at five different locations: two reefs (R1 and R2), their associated surrounding sponge grounds (S1 and S2), and one control site with bare soft sediments (C). The control site did not host corals or sponges, and was located at a similar water depth, east of the Træna Coral MPA (**Figure 1B**).

CWCR in the Træna area are aligned along the main westward current direction (Laberg et al., 2002) and are typically composed of three distinct parts: a "head" part with living coral, a "middle" section with dead coral framework, and a long "tail" part, which consists primarily of coral rubble (**Figure 1C**). The reef's head part faces the current and consists of several meters wide vertically-oriented lobes, primarily composed of living *Lophelia pertusa,* (Buhl-Mortensen et al., 2010, **Figure 2D**). The sponge ground sites were located in the vicinity of the reef sites and were dominated by three sponge types: *Mycale lingua*, *Oceanapia* spp., and Geodiidea (Kutti et al., 2013).

Biological Data on Corals and Sponges

We determined the coral polyp density from ROV video transects at site R1 (**Table 2**) along three different lobes of live Lophelia. The number of "visible" polyps per square meter was estimated on calibrated (i.e., corrected for the view angle of the camera) still images taken from the video. To this end, we delineated 3–4 squares of 10 cm by 10 cm in a single video image and counted the number of "visible" polyps within these reference squares.

By comparing the number of living polyps on intact coral branches collected by the ROV with the number of living polyps

TABLE 1 | Station locations and instrument deployments.

Date	Longitude (°W)	Latitude (°N)	Type of habitat	Instrument	Type of measurement
27.05.2011	11 ° 26.27	66 ° 56.13	Bare sediment	AqEC	*In situ* CR
27.05.2011	11 ° 26.72	66 ° 56.35	Bare sediment	Box corer	3 onboard incubations of sediment cores
28.05.2011	11 ° 07.76	66 ° 58.31	Coral reef R1	ROV	Sampling of *Lophelia* branches followed by on-board incubation
28.05.2011	11 ° 07.95	66 ° 58.44	Coral reef R1	Box corer	3 core incubations
29.05.2011	11 ° 05.94	66 ° 58.44	Coral reef R1	AqEC	*In situ* CR
29.05.2011	10 ° 58.45	66 ° 58.20	Sponge groundS1	ROV	Geodia collection + incubation
29.05.2011	11 ° 06.05	66 ° 58.43	Coral reef R1	Box corer	2 core incubations
29.05.2011	11 ° 06.12	66 ° 58.44	Sponge ground S1	AqEC	*In situ* CR
29.05.2001	11 ° 06.48	66 ° 58.44	Coral reef R2	AqEC	*In situ* CR
29.05.2011	11 ° 06.12	66 ° 58.44	Sponge ground S1	Box corer	2 core incubations
30.05.2011	11 ° 06.66	66 ° 58.44	Sponge ground S2	AqEC	*In situ* CR
30.05.2011	11 ° 06.59	66 ° 58.44	Coral reef R2	Box corer	2 core incubations
30.05.2011	11 ° 06.66	66 ° 58.44	Sponge ground S2	Box corer	2 core incubations

AqEC, Aquatic Eddy Correlation; CR, Community Respiration; ROV, Remotely Operated Vehicle.

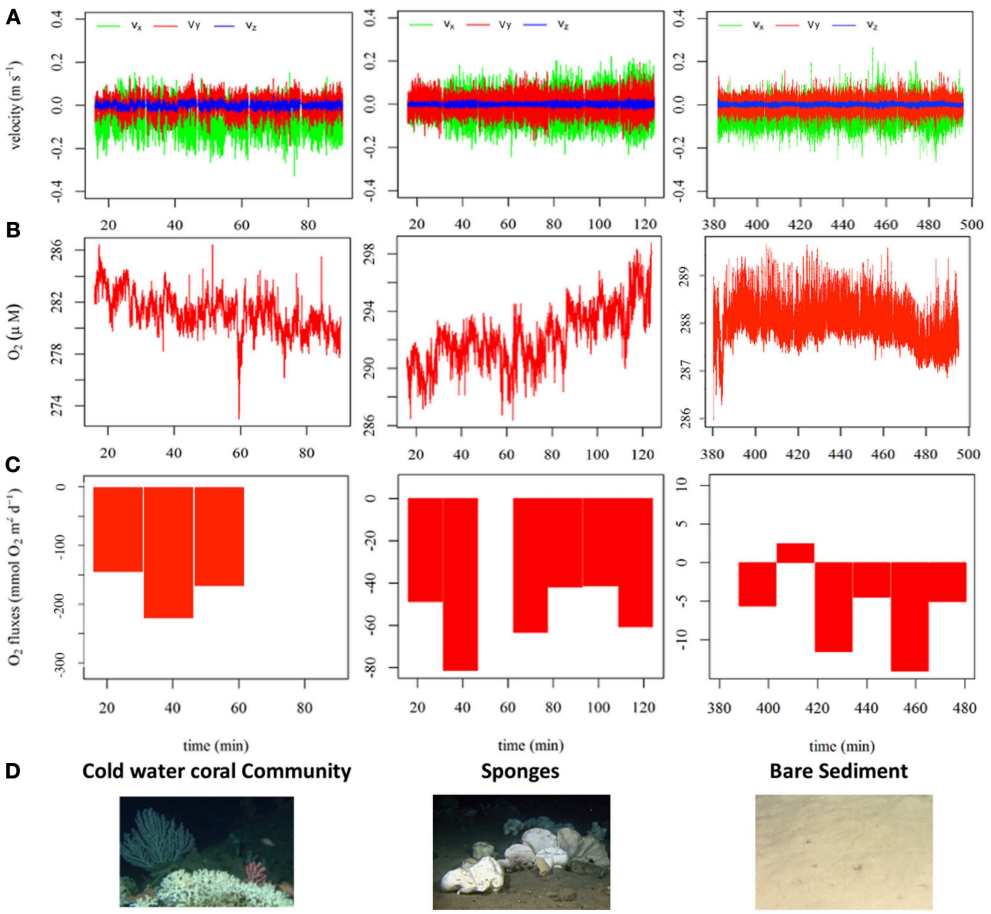

FIGURE 2 | AqEC correlation data for consecutive 15 min bursts during the deployment at the reef R1, sponge ground and bare sediment sites. (A) Velocity data (x, y, z) after a 3 Hz low-pass filtering. **(B)** Raw O_2 concentration data after a 3 Hz low-pass filtering. **(C)** Derived O_2 flux for each burst (rectangles). **(D)** Images of the corresponding habitats and associated communities (Cold water coral, sponges and bare sediment).

that were visible on single branches in calibrated ROV video images, we estimated that 80 ± 10% of the living polyps were hidden from view on the ROV video images (**Figure 1E**). We hence multiplied the "visible" polyp density estimated from the ROV video images by a factor of 5 to arrive at the true areal density of living *L. pertusa* polyps.

We estimated the abundance of the four main sponges (*Geodia barretti*, *G. atlantica*, *G. macandrewii*, and other *Porifera*) by analyzing images of an ROV survey (HL5-5) carried out in 2009 at site S1 (Kutti et al., 2013). In each image, individual sponges were taxonomically identified and their density (ind m^{-2}) and individual size (length, diameter) was estimated.

In addition, a scaling relation was derived between the volume and biomass of *Geodia barretti* (**Table 3**) to estimate the total sponge biomass. During the cruise, five specimen of *G. barretti* were collected with the ROV, and their individual volume (through water displacement) and wet weight was measured. Dry weight biomass was calculated from wet weight using a 0.2 conversion factor determined from previous measurements on Geodia sponges (Tjensvoll et al., 2013; Kutti et al., 2014).

Eddy Correlation *in situ* Community Respiration Measurements

Five deployments were performed within the three habitat types (1 in soft-sediment, 2 in sponge ground and 2 in coral reef habitat) using a tripod lander, which carried the Aquatic Eddy Covariance (AqEC) instrument and which was launched from the research vessel (**Table 1**). The AqEC flux technique is based on the simultaneous high-frequency measurement of the current velocity vector u and the oxygen concentration C at a given height above the seabed, from which the turbulent fluctuations in the oxygen concentration C′ and in vertical current velocity u'_z are calculated. The oxygen flux toward the seabed is subsequently obtained as the temporal average of the covariance $\overline{u'_z\, C'}$ (Berg et al., 2003, 2009). The AqEC instrument consisted of an Acoustic Doppler Velocimeter (ADV, Vector Nortek®) and a fast-responding Clark-type O_2 microelectrode directly connected to an auto-zeroing amplifier (Unisense®, Denmark). Both the ADV and the O_2 sensor were interfaced to a controller unit (Unisense®, Denmark), which took care of power supply, sensor synchronization and data storage. The O_2 sensors (Unisense®, Denmark) had an outer tip diameter of ∼5 µm, and a response

time of ∼0.3 s. The O_2 sensor was polarized for at least 6 h prior to use and a two-point calibrated was carried out using saturated bottom water (100% reference) and an oxygen-free solution of 1 M Na-ascorbate and 0.5 M NaOH (0% reference).

The AqEC instrument was mounted on a tripod bottom lander equipped with a vane attached to one leg of the lander, which ensured that the O_2 sensor faced the direction of the main current (**Figure 1**). Visual inspection by the ROV confirmed the correct positioning of the AqEC lander on the reef framework. In all deployments, the sensor volume of the ADV was positioned 35–45 cm above the sediment-water interface. AqEC deployments typically lasted 2 h, except for the deployment in the bare sediment control area, which lasted 24 h. During this 24 h deployment, we selected 2 h (8 bursts) of data that passed quality control criteria (see details below). Data collection always proceeded in 15 min bursts, each consisting of a 14 min period of data recording at 64 Hz, followed by a 1 min pause.

TABLE 2 | Polyp density of Reef R1 based on ROV video survey images.

Lobe	No. of polyps on image per 10 × 10 cm^2 area	No. of polyps m^{-2}	
1	23	1668	
1	35	2538	
1	33	2393	
1	32	2320	
2	36	2610	
2	26	1885	
2	36	2610	
3	30	2175	
3	40	2900	Considering 5 layers of polyps
3	40	2900	
Average	33.1 ± 5.6	2400 ± 400	12000 ± 2000

n.b., Number of polyps were estimated based on calibrated snapshots (factor: 0.725).

AqEC data time series were pre-processed using a dedicated R script developed at NIOZ, which involved de-spiking of the oxygen and velocity data, followed by a two-axis rotation of the velocity data (Mcginnis et al., 2008). In case of the reef deployments, we applied a planar fit rotation to the velocity data in order not to make any further assumptions on the flow field, and to examine the occurrence of any flow divergence that might generate spurious fluxes. A low-pass filter (3 Hz) was applied to the vertical velocity data to remove high-frequency noise. In oceanic environments, flux contributions are typically below 1 Hz (Lorrai et al., 2010), and we verified that our low-pass filtering did not affect the calculated fluxes.

In AqEC studies, three methods have been used to obtain the fluctuating components of the vertical velocity and oxygen (mean removal, linear detrending, and running mean filtering). In this study, we implemented running mean filtering because it gave the best linear cumulative fluxes (please see below). To this end, the mean velocity and oxygen concentration were calculated as the running means obtained by applying a 1/60 Hz high-pass filter to the 3 Hz filtered data in each burst. Referring to these running means as $\overline{u_z}$ and $\overline{C_z}$, values of u_z' and C' were then calculated as $u_z - \overline{u_z}$ and $C - \overline{C_z}$ where u_z and C represent the 3 Hz filtered data. The AqEC flux was then calculated as the mean covariance over the time domain of each burst together with the associated cumulative flux. The cumulative flux is simply the value of the instantaneous AqEc flux ($u_z'C'$), which is integrated over time. If $u_z'C'$ is constant in time, this cumulative flux should increase in a linear way throughout each burst. Hence, the cumulative flux was visually inspected to reflect a steady linear uptake of O_2 by the seafloor during the respective bursts. If the cumulative flux did not display a sufficiently linear trend ($r^2 < 0.6$), the burst was discarded. A fast Fourier transformation of u_z' and C' provides the individual spectra as well as the co-spectrum, which expresses the flux contribution as a function of the eddy frequency (Berg et al., 2003). After careful examination of the variance preserving co-spectra of each burst, the use of a 60 s averaging time period was selected (i.e., 1/60 Hz high-pass filter

TABLE 3 | Estimation of the sponge density and biomass from ROV video survey images and of respiration rates.

	Average density	Average Diameter	Biomass*	Biomass §	Respiration rates†	CR rates
	(ind m^{-2})	*(cm)*	*(kg WW m^{-2})*	*(kg DW m^{-2})*	*(mmolO_2 g DW d^{-1})*	*(mmolO_2 m^{-2} d^{-1})*
Geodia barretti	0.24	29	3.2 ± 1.5	0.63 ± 0.3	0.036	23.0 ± 10.8
G. atlantica	0.07	53	0.8 ± 0.4	0.16 ± 0.08	0.036	5.8 ± 2.9
G. macandrewii	0.02	24	0.3 ± 0.1	0.06 ± 0.02	0.036	2.2 ± 0.7
Porifera indet.	0.22	19	2 ± 0.9	0.4 ± 0.2	0.036	14.4 ± 6.5
Total community of massive sponges	0.55		6.3 ± 2.9	1.3 ± 0.6	0.036	45.3 ± 20.9
					Sponge sediment	3.4 ± 0.6
					Total	48.7 ± 21.5

**Biomass was calculated for each individual using the size-weight conversion factor measured for G. barretti, i.e., biomass = 0.0003 × length^3 (Kutti et al., 2013). §Conversion factor of 0.20 was used to convert from wet weight to dry weight biomass. †The respiration rate obtained for G. barretti was used also to estimate oxygen consumption of the other massive sponges.*

as noted above) ensuring that the lowest frequencies contributing to the flux are accounted for.

Quality control of the AqEC time series data is crucial for accurate flux extraction. Each burst was examined separately and the burst data were discarded if (1) ADV data were of insufficient quality (beam correlation values below 70%), (2) the current velocity and oxygen concentration showed any sign of statistical non-stationarity (by investigating changes in the mean and standard deviation of C and u_z over time) or (3) storage effects were noted (by monitoring the oxygen inventory between sediment and the O_2 sensor position) (4) the cumulative flux was not sufficiently linear (Reba et al., 2009; Hume et al., 2011; Lorke et al., 2013). Hence, the entire 2 h data-sets for the reefs and sponges deployments, and the entire 24 h datasets for the sediment control deployment, were visually inspected for subsets with stationary conditions: we ensure that burst averaged velocity and concentrations showed only limited changes over time. For instance, on reef 1, burst averaged horizontal velocities vx in those stationary subsets ranged from −0.06 to 0 m s^{-1} and burst averaged oxygen concentrations ranged from 268 to 281 μM. Burst-to-burst changes of averaged oxygen concentrations were maximum 4 μM, which allowed us to disregard potential storage effects (Lorke et al., 2013). Additionally, each 15 min burst was examined separately. Bursts with clear artifacts in data (such as abrupt changes in averages of subsections) where discarded, as well as bursts where the cross correlation function did not show a clear minimum or maximum but was either entirely erratic or showed multiple extrema over the −100 - +100 s time lag. When the cumulative fluxes showed a random-walk like behavior rather than a linear trend, we co-examined the co-spectra, ogives, cross-correlation function and discarded the burst if they all presented significant anomalies.

We used the cross correlation among the horizontal u_x and u_y and vertical u_z velocity components to calculate the friction velocity (Kim et al., 2000), and this way, we could assess a rough estimate for the footprint area of our AqEC measurements (Berg et al., 2007). This calculation revealed that footprints covered an area about 10–25 m long and 2.3–2.9 m wide in the various deployments.

Incubation-Based Community Respiration Rates

Living coral branches (*Lophelia pertusa*) and dead coral branches (*Lophelia pertusa*) were collected by the ROV and their oxygen consumption rates were determined by closed chamber incubations (**Table 1**).

Coral fragments were placed in acrylic chambers (I.D. 10 cm) filled with filtered (50 μm pore size) bottom water collected by a CTD rosette sampler. Chambers were then closed with a lid equipped with a magnetic stirrer, temperature and oxygen sensors (FIBOX oxygen optode, PreSens Gmbh). Incubations were performed in the dark at *in situ* temperature in a temperature-controlled shipboard incubator. Temperature and oxygen concentrations were continuously logged during incubations. Oxygen concentrations in the chamber were additionally determined at the beginning and end of each incubation via Winkler titration (Grasshoff, 1976). Oxygen consumption rates were computed by linear regression of the oxygen concentration data over the first period of the incubations (total O_2 decrease < 20%). The O_2 consumption rate of intact bare sediment substrate was determined in a similar way, using intact sediment cores subsampled from the box-core. The duration of the incubations was 7.9 ± 2.6 h, and the O_2 concentrations had by then dropped on average by 13%. On-board respiration rates for sponges (*Geodia barretti*) were obtained in a similar way, using larger incubation chambers, yet during earlier cruises (transect HL5-5, in Kutti et al., 2013).

To validate the AqEC measurements, whole ecosystem respiration rates were estimated in a "bottom-up approach" by suitably combining the respiration rates of separate habitat components and upscaling these within the footprint area of the AqEC instrument. This procedure was applied to the 3 habitats (coral reef, sponge ground, and soft-sediment) where the AqEC lander was deployed.

Soft-sediment community respiration (CR) rates were considered as directly equal to the rates obtained by incubating the sediment substrate.

Sponge CR rates were calculated as the soft-sediment CR rates summed with the sponges incubation-based respiration rates. Indeed, we considered the sponge ground ecosystem as the sum "sponges + sediment."

Coral reef community respiration (CR) rates were calculated as the area-weighted mean of the four main habitat types that covered the AqEC footprint area: (1) live Lophelia, (2) mixed and dead Lophelia framework, (3) dead coral framework, and (4) coral rubble. To determine the contribution of each habitat type, ROV video transects were carried out over site R1 from the AqEC deployment location up to the head part of the reef (thus mapping the habitat variation in the footprint area of the AqEC instrument along the longitudinal axis of the reef). To each habitat type, we subsequently assigned a specific community respiration rate. Respiration rates of dead coral framework and coral rubble were obtained as described above for the coral branches collected by the ROV. To estimate respiration rate of the live Lophelia habitat, we accounted for the 3D structure of the reef and the whole polyp activity: we counted the polyps on the incubated living coral branches and normalized the oxygen consumption rates by the number of polyps. Live Lophelia respiration rates were hence calculated as the polyp normalized live respiration rate (i.e., oxygen consumption rate per polyp) multiplied by the polyp density of the reef estimated through the ROV transect (i.e., number of polyp per square meter) and corrected from the 5 layers of polyps (multiplied by 5, see above).

Upscaling Procedures of the CR Rates

Both of our AqEC and bottom up CR rates were upscaled over the entire coral reefs by considering the cigar shape of the reefs and based on 3D reconstruction of reef 1 from the ROV images and the positioning of the EC lander (see Supplementary Materials, length: 125 m, width: 45 m). The reefs were modeled as two joint domains (see Supplementary Materials): one dominated by live corals (area A1: 1767 m^2,), and the other one dominated by dead coral framework and coral rubble sediment (area A2: 1688 m^2). Reef CR rates, calculated above, were taken as representative of the domain A1, whereas sediment CR rates were taken as

representative for domain A2. Upscaled CR rates were then calculated as the area weighted mean using the following formula:

$$\text{Upscaled CRflux} = \frac{\begin{array}{c}\text{Coral flux*area A1}\\ +\text{Sediment flux*area A2}\end{array}}{\text{area A1} + \text{area A2}}$$

For larger scale considerations and regional estimates of CR rates over reef and sponge beds, we chose to consider only the rates obtained by the AqEC technique, in order to take a more integrated value of the ecosystem. For the sediment control area however, we chose to average the rates obtained by both techniques, since AqEC and incubation would give a representative estimate of the CR rates.

Error Propagation and Statistical Differences

Statistical differences between the AqEC and bottom-up techniques were tested among the three habitats using the Wilcoxon rank signed sum-test.

In the error propagation, we accounted for the standard deviation of fluxes using standard basic rules (please refer for instance to http://www.rit.edu/cos/uphysics/uncertainties/Uncertaintiespart2.html).

Hence, taking into account the associated standard deviation of the fluxes, we calculated the average between (i) AqEC fluxes measured over identical habitats (e.g., reefs R1 and R2, sponge grounds S1 and S2), (ii) incubations based CR of different coral compartments, and iii) AqEC and incubation based CR over sediment area.

Results

Reef Habitat Composition

The seafloor in the Træna Deep Coral reef field (Norwegian continental shelf) comprises three main habitat types (Buhl-Mortensen et al., 2010; Kutti et al., 2013): (i) elongated, cigar-shaped reefs (100–150 m long, 25–55 m wide and on average 7 m high) formed by the reef-building coral *Lophelia pertusa*, (ii) dense sponge grounds surrounding the coral reefs, consisting of aggregations of large demosponges, and (iii) stretches of bare sediment away from the reefs, containing typical soft-sediment infauna. Video transects in the footprint area of the AqEC lander at the Reef site R1 revealed a mosaic of four main reef habitat types: live coral framework (covering 53% of the transect), mixed live and dead coral framework (8%), dead coral framework (12%), and coral rubble (27%) (**Table 4**).

Community Respiration (CR) Rates

Representative data time series obtained during AqEC deployments for the three habitat types (reef R1, sponge ground S1 and control bare sediment C) are shown in **Figure 2**. Community Respiration (CR) rates, obtained by AqEC, differed by two orders of magnitude between the three habitats, revealing strong differences in carbon processing rates (**Figure 3**). The AqEC-based CR of the bare sediment site was 6 ± 2 mmol O_2 m^{-2} d^{-1} and compared favorably to CR obtained from shipboard incubations of sediment cores (3 ± 1 mmol O_2 m^{-2} d^{-1}). These low CR values are also consistent with rates ($\approx$1 mmolO_2 m^{-2} d^{-1}) previously reported for the Norwegian continental shelf at comparable water depths (Graf et al., 1995). AqEC-based CR rates within the sponge grounds were $\sim$10 times higher (54 ± 5 mmol O_2 m^{-2} d^{-1}) than the bare sediment rates and compared well with the bottom-up estimate at the sponge ground site (48.7 ± 21.5 mmol O_2 m^{-2} d^{-1}), which was obtained by combining and integrating the individual respiration contributions of different habitat types within the AqEC footprint area (**Table 3**). CR rates over the coral reef were systematically higher than in the adjacent bare sediments and sponge grounds (**Figure 3**). The highest AqEC-based CR rates (246 ± 18 and 177 ± 40 mmol O_2 m^{-2} d^{-1}) were obtained during the deployments on the head part of the reef, which is densely covered with living *Lophelia pertusa* (**Figures 1B,D**). The bottom-up CR estimates over CWCR (82 ± 10 mmol O_2 m^{-2} d^{-1}; **Table 4**) are about 40% of these AqEC fluxes. However, comparing the two AqEC and bottom-up methods over the 5 deployments (i.e., all 3 habitats), CR rates were not statistically different ($p = 0.25$, $n = 5$). Upscaling our AqEC measurements to the whole reef structure (including the downstream tail part that is less metabolically active) provided an average CR rate of 122 ± 10 mmol O_2 m^{-2} d^{-1} (**Table 5**), whereas upscaled bottom-up CR rates gave a value of 43 ± 7 mmol O_2 m^{-2} d^{-1}. Ratios between the reef and the sediment CR rates were 20 and 14, respectively for the AqEC and bottom-up technique. For the sponge habitat, ratios were of 9 and 16, respectively for the AqEC and bottom-up estimates.

Discussion

Despite the complex topography of the reef structure and the substantial uncertainty associated with the "bottom-up" CR rates, the AqEC and bottom-up values align very well, and are not significantly different for the sponge ground and bare sediment. However, AqEC technique did provide significantly higher CR rates than the "bottom-up" incubation method over the reef habitats (**Figure 3**). This difference can be either due to an overestimation on behalf of the AqEC technique, or equally, an underestimation associated with the bottom up incubation approach. Clearly, the bottom-up approach requires a whole series of upscaling steps, where each upscaling step introduces a new set of parameters (e.g., polyp density, local habitat cover), which each are associated with a given uncertainty. These uncertainties eventually propagate through the upscaling process, which creates the possibility for a substantial uncertainty on the final community respiration rate. On the other hand, the application of the AqEC technique over a topographically complex habitat, such as a cold-water coral reef, is also challenging, and one should be vigilant that the basal assumptions underlying the AqEC technique are still satisfied. One critical assumption is that flow convergence or flow divergence are negligible, which is not necessarily the case in an environment with complex and rough topography, such as coral reefs and sponge grounds. When present, flow convergence/divergence may induce vertical velocity variations that can induce higher, spurious fluxes (Reimers et al., 2012;

TABLE 4 | Structure and Community Respiration (CR) rates of Reef R1 based on ROV video survey images and incubation rates.

Compartment		Respiration rate ($mmolO_2\ m^{-2}\ d^{-1}$)
Living coral	A	77.0 ± 12.8
Dead coral	B	13.7 ± 1.6
Coral rubble	C	3.3 ± 1.0

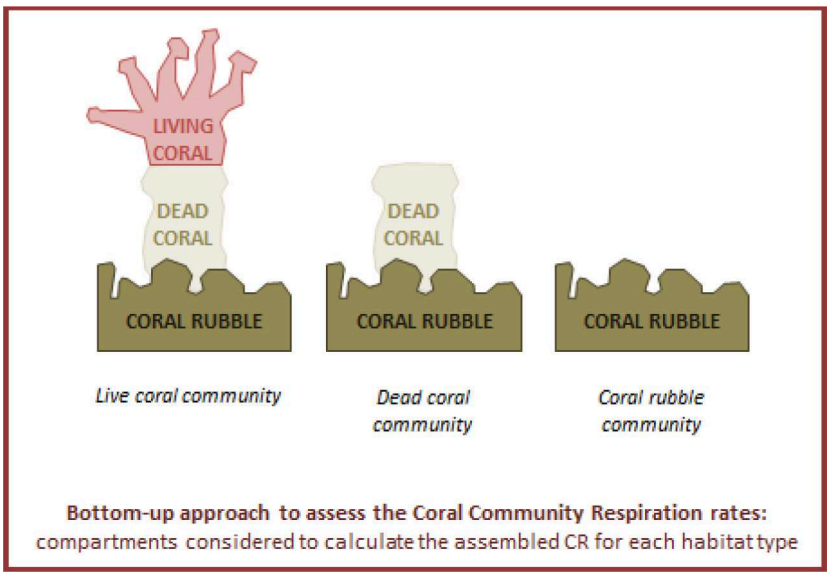

Habitat type	Aeral contribution (%)	Formula	Habitat CR rates ($mmolO_2\ m^{-2}\ d^{-1}$)	Aeral coral CR rates ($mmolO_2\ m^{-2}\ d^{-1}$)
Live coral	53	$A+B+C$	139.2 ± 18.3	73.8 ± 9.7
Mixed live and dead coral framework	8	$\frac{(A+B)}{2}+B+C$	62.2 ± 13.1	5.0 ± 1.0
Dead coral framework	12	$B+C$	16.9 ± 1.9	2.0 ± 0.2
Coral rubble	27	C	3.3 ± 1.0	0.9 ± 0.3
			Total	81.7 ± 9.8

Each habitat CR rates is calculated as the sum of its different compartments (Formula). Areal habitat CR rates are each individual habitat CR rates scaled-up to the entire reef using their respective surface area contribution.

Lorke et al., 2013). We specifically assessed the importance of flow divergence at the reef site, by implementing a planar fit rotation to the ADV velocity data. This coordinate rotation aligns the mean horizontal velocity along the main streamline and hence one does not need to invoke any assumption regarding the flow field (Lorke et al., 2013). We found that the AqEC fluxes did not change after the application of the planar fit rotation, which hence suggests a negligible impact of flow divergence on the fluxes. Moreover, hydraulic studies examining the influence of forward facing steps on the flow pattern (Ren and Wu, 2011), have shown that for similar Reynolds numbers (Re ∼400) as over the reefs, the effect of flow divergence becomes negligible after ∼1.5 times the length of the step (in our case about 7 * 1.5 = 10.5 m, while the AqEC lander here was positioned 20 meters behind the 7 meter step increase). Accordingly, we believe that flux divergence was most likely negligible in our reef measurement, but future studies could however consider a more detailed and more extensive evaluation of the AqEC technique in topographically complex environments like coral reefs (e.g., by placing multiple instruments in parallel, or examining whether the flux at different sensor heights).

Both the bottom-up approach and the AqEC methods show that the CR rates on the reef and sponge grounds are substantially elevated compared to the bare sediment control site. These high CR rates evidently suggest intensified organic processing within the CWCR and sponge grounds of the Traena MPA. Based on our AqEC rates (which we consider more reliable than the corresponding bottom up estimates), community respiration in CWCR and sponge grounds are, respectively, ∼20 and ∼9 times higher than those of the surrounding soft sediments. The observation that CWCR and sponge grounds function as hotspots of respiration is supported by indirect estimates of community respiration at other locations in the North Atlantic (Van Oevelen et al., 2009; White et al., 2012). Recently, Rovelli et al. (2015) reported respiration rates up to 46 mmol O_2 m^{-2} d^{-1} in CWCR habitats in the Stjernsund area on the Norwegian shelf, which were also significantly higher than within adjacent bare sediment areas. If we compare the few available data against a global compilation of soft sediment data, CWCR and sponge grounds clearly stand out by their high community respiration rates (**Figure 4**), although it is clear that there is variability among the few CR rates available in the literature. Indeed, CWCR and sponge ground sites can differ significantly both in terms in

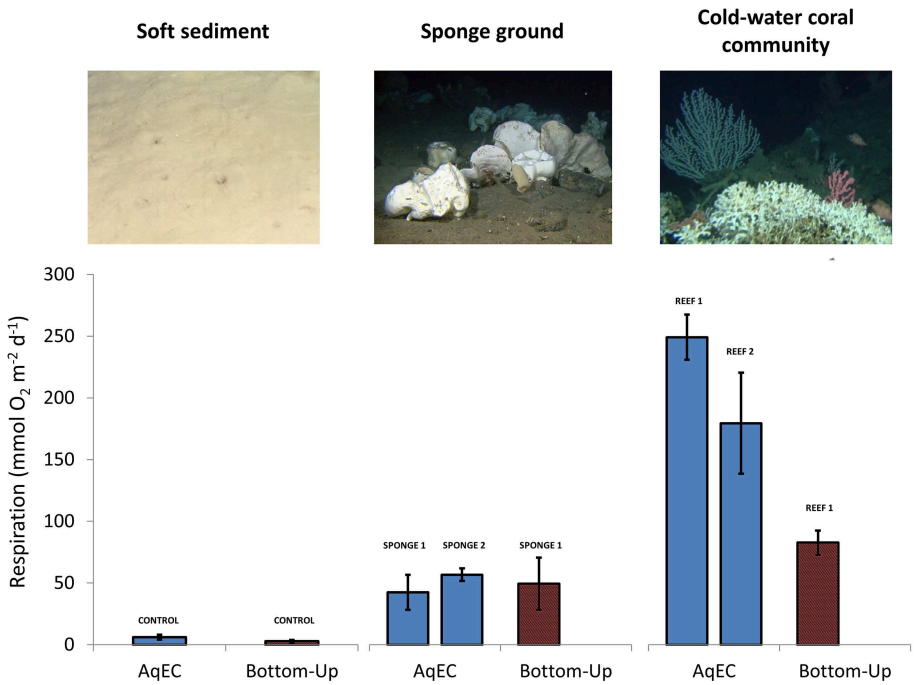

FIGURE 3 | Community respiration rates in bare sediment (left), sponge ground (center), and cold-water coral reef (right). AqEC, Aquatic Eddy Correlation. Bottom-up, Bottom-up community respiration rate. AqEC fluxes correspond to separate deployments over two reefs, two sponge fields and one bare sediment control area (**Figure 1B**). Error bars indicate standard deviations for AqEC fluxes and propagated errors for the bottom-up estimates. Names above the bars indicate where the measurement was performed.

density and structure, impacting the absolute values of the CR rates between different sampling sites. However, the common feature of CWCR and sponge field among all studies is their carbon processing rates significantly higher than the surrounding environments (**Figure 4**).

The high metabolic activity of CWCR and sponge grounds has important implications for carbon cycling and benthic-pelagic coupling at the regional scale of the Træna MPA, but also at the wider scale of the Norwegian continental shelf (**Table 5**). Using the CR rates obtained here, and considering a ∼22% seafloor coverage (Lindberg, 2004; Kutti et al., 2013), CWCR and sponge grounds account for 78% of the total benthic respiration, and consume 63% of the total OC export flux in the Træna MPA (Slagstad et al., 1999). CWCR habitats cover ∼1671 km^2 of the Norwegian continental shelf (150.000 km^2, Fossa et al., 2002), while recent ROV observations suggest at least a similar coverage for sponges (Cruise report, R/V Håkon Mosby—cruise #2009615). Using these estimates of seafloor coverage, CWCR and sponge grounds are jointly responsible for 36% of the total benthic respiration on the Norwegian continental shelf, and process 5% of the total primary production in the area (Schluter et al., 2000). Conventional carbon budgets typically only account for soft-sediment respiration and hence, these budgets may significantly underestimate total seafloor carbon cycling and the intensity of the benthic-pelagic coupling on continental shelves with coral and sponge reefs.

The intense metabolic activity of CWCR and sponge grounds can only be maintained through a local focusing of the downward export flux of detritus from the surface ocean. CWCR are frequently reported from sites with locally accelerated currents, along margins with enhanced down-slope particle transport, or where internal tidal waves facilitate and increase the seabed food supply (Roberts and Cairns, 2014). The carbonate framework baffles currents and enhances organic matter trapping, thus providing a detritus-focusing mechanism. This way, CWCR act as ecosystem engineers, directly modulating the availability of resources to their surrounding environment (Mienis et al., 2009; Van Oevelen et al., 2009). Compared to corals, sponges form smaller, decimeter-sized, structures on the seafloor, but are known for their impressive filtration capacity. In the Træna MPA, the local sponge community has been estimated to filter about 1 m of the benthic boundary layer each day (Kutti et al., 2013). We hypothesize that the focusing of the OC export flux onto CWCR and sponges, through organic matter trapping and filtration (Kutti et al., 2013), will reduce the detritus input to the peripheral soft-sediment communities, impacting the local biodiversity and carbon cycling. By dominating benthic OC processing in Træna MPA, CWCR and sponge grounds will also influence regional ecosystem functions, such as carbon storage and nutrient recycling. As a consequence, future seafloor carbon budgets should account for the intense biogeochemical cycling in CWCR and sponge grounds. Moreover, the interplay between the high respiration activity described here, and the anticipated

TABLE 5 | Carbon budget over the Traena Marine Protected Area (MPA), and the Norwegian Continental Shelf.

	Benthic oxygen uptake rate*			Benthic carbon uptake rate+			Area	C demand			% Resp	% Export OC†
	$mmolO_2 m^{-2} d^{-1}$			$gC\ m^{-2}\ y^{-1}$			km^2	$10^3\ tC\ y^{-1}$			%	%
	avg		std	avg		std		avg		std		
							Traena MPA					
Bare sediment	3.6	±	0.9	12.0	±	3.0	251	3.0	±	0.8	21.5	17.3
CWCR	121.5	±	9.9	408.6	±	33.2	4	1.5	±	0.1	10.7	8.6
Sponges	54.4	±	4.7	183.1	±	15.8	52	9.5	±	0.8	67.7	54.4
							Total	307	14			
							Norwegian continental shelf				% Resp	% PP‡
							Bare sediment	146658	1764	± 439	63.5	10.3
							CWCR	1671[a]	683	± 55	25.2	4.1
							Sponges	1671[b]	306	± 26	11.3	1.8
							Total	150000[c]	2753			

*Comparison between the AqEC respiration rates and the Organic Carbon (OC) export flux and Primary Production (PP). *Benthic respiration rates based on our AqEC measurements. Benthic oxygen uptake for bare sediment was however calculated as the average of our AqEC fluxes and bottom-up rates taking into account the variance of each (see the error propagation section). +Respiratory quotient: 0.77 (Froelich et al., 1979). †Total export flux: 57 $gC\,m^{-2}\ y^{-1}$ (Slagstad et al., 1999). ‡Primary Production: 112.7 $gC\ m^{-2}\ y^{-1}$ (Schluter et al., 2000).*

[a] *From (Fossa et al., 2002).*

[b] *Based on (Klitgaard and Tendal, 2004), we assumed a similar coverage for sponges than for corals.*

[c] *From (Schluter et al., 2000; Huthnance, 2010).*

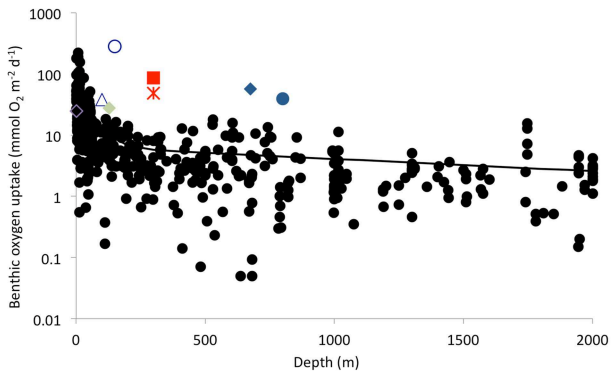

FIGURE 4 | Community Respiration Rates in cold-water coral reefs plotted against a compilation of soft sediment data (•) as a function of water depth. Tisler Reef (△) (Wagner et al., 2011)—Rockall Bank (◆) (Van Oevelen et al., 2009)—Mingulay Reef (○) (Maier et al., 2009)—Hatton Bank (●, Van Oevelen, unpublished data)—Træna Reef ■, this study)—Mingulay Reef (◆) (Rovelli et al., 2015)—Stjernsund (◇) (Rovelli et al., 2015). Sponge ground data for Tranea reef are also included (✱). The solid line shows an empirical model fit (double-exponential decrease with water depth) to the compiled soft sediment data (Andersson et al., 2004).

climate feedbacks on organic matter export from the surface ocean flux (Bopp et al., 2001), emphasize the sensitivity of deep-sea communities to climate change (Roberts and Cairns, 2014).

Author Contributions

GD, DV, and FM designed the study. CC performed AqEC measurements. CC and TC analyzed the AqEC output data. ML and DV performed ship-board respiration incubations. TK performed sponge respiration rates measurements and analysis of ROV images. CC, DV, and FM wrote the manuscript. All authors contributed substantially to the discussion of the results and revision of the manuscript.

Acknowledgments

We thank the crew and technical assistants of the RV Håkon Mosby for their support at sea and during the operation of the ROV Aglanta. This research was funded by CoralFISH, a project in the European Community's Seventh Framework Programme (FP7/ 2007-2013) under grant agreement number 213144, Odysseus grant G.0929.08 (FWO, Belgium) to FJRM, VIDI grant 864.08.004 (NWO, The Netherlands) to FJRM and VIDI grant 864.13.007 (NWO, The Netherlands) to DV.

Supplementary Material

The Supplementary Material for this article can be found online at: http://journal.frontiersin.org/article/10.3389/fmars.2015.00037/abstract

References

Althaus, F., Williams, A., Schlacher, T. A., Kloser, R. J., Green, M. A., Barker, B. A., et al. (2009). Impacts of bottom trawling on deep-coral ecosystems of seamounts are long-lasting. *Mar. Ecol. Prog. Ser.* 397, 279–294. doi: 10.3354/meps08248

Andersson, J. H., Wijsman, J. W. M., Herman, P. M. J., Middelburg, J. J., Soetaert, K., and Heip, C. (2004). Respiration patterns in the deep ocean. *Geophys. Res. Lett.* 31, L03304. doi: 10.1029/2003GL018756

Attard, K. M., Glud, R. N., Mcginnis, D., and Rysgaard, S. (2014). Seasonal rates of benthic primary production in a Greenland fjord measured by aquatic eddy correlation. *Limnol. Oceanogr.* 59, 1555–1569. doi: 10.4319/lo.2014.59.5.1555

Berg, P., Glud, R. N., Hume, A., Ståhl, H., Oguri, K., Meyer, V., et al. (2009). Eddy correlation measurements of oxygen uptake in deep ocean sediments. *Limnol. Oceanogr. Methods* 7, 576–584. doi: 10.4319/lom.2009.7.576

Berg, P., Røy, H., Janssen, F., Meyer, V., Jørgensen, B. B., Huettel, M., et al. (2003). Oxygen uptake by aquatic sediments measured with a novel non-invasive eddy-correlation technique. *Mar. Ecol. Prog. Ser.* 261, 75–83. doi: 10.3354/meps261075

Berg, P., Roy, H., and Wiberg, P. L. (2007). Eddy correlation flux measurements: the sediment surface area that contributes to the flux. *Limnol. Oceanogr.* 52, 1672–1684. doi: 10.4319/lo.2007.52.4.1672

Bopp, L., Monfray, P., Aumont, O., Dufresne, J. L., Le Treut, H., Madec, G., et al. (2001). Potential impact of climate change on marine export production. *Global Biogeochem. Cycles* 15, 81–99. doi: 10.1029/1999GB001256

Buhl-Mortensen, L., Vanreusel, A., Gooday, A. J., Levin, L. A., Priede, I. G., Buhl-Mortensen, P., et al. (2010). Biological structures as a source of habitat heterogeneity and biodiversity on the deep ocean margins. *Mar. Ecol. Evolut. Perspect.* 31, 21–50. doi: 10.1111/j.1439-0485.2010.00359.x

Dodds, L. A., Roberts, J. M., Taylor, A. C., and Marubini, F. (2007). Metabolic tolerance of the cold-water coral *Lophelia pertusa* (Scleractinia) to temperature and dissolved oxygen change. *J. Exp. Mar. Biol. Ecol.* 349, 205–214. doi: 10.1016/j.jembe.2007.05.013

Fisher, C. R., Hsing, P.-Y., Kaiser, C. L., Yoerger, D. R., Roberts, H. H., Shedd, W. W., et al. (2014). Footprint of Deepwater Horizon blowout impact to deep-water coral communities. *Proc. Natl. Acad. Sci. U.S.A.* 111, 11744–11749. doi: 10.1073/pnas.1403492111

Fossa, J. H., Mortensen, P. B., and Furevik, D. M. (2002). The deep-water coral *Lophelia pertusa* in Norwegian waters: distribution and fishery impacts. *Hydrobiologia* 471, 1–12. doi: 10.1023/A:1016504430684

Froelich, P. N., Klinkhammer, G. P., Bender, M. L., Luedtke, N. A., Heath, G. R.;, Cullen, D., et al. (1979). Early oxidation of organic matter in pelagic sediments of the eastern equatorial Atlantic: suboxic diagenesis. *Geochim. Cosmochim. Acta* 43, 1075–1090. doi: 10.1016/0016-7037(79)90095-4

Graf, G., Gerlach, S. A., Ritzrau, W., Scheltz, A., Linke, P., Thomsen, L., et al. (1995). Benthic-pelagic coupling in the Greenland Norwegian Sea and its effect on the geological record. *Geologische Rundschau* 84, 49–58. doi: 10.1007/BF00192241

Grasshoff, K. (ed.). (1976). *Methods of Seawater Analysis*. Weinheim; New York: Verlag Chemie.

Hume, A., Berg, P., and McGlathery, K. J. (2011). Dissolved oxygen fluxes and ecosystem metabolism in an eelgrass (Zostera *marina)* meadow measured with the eddy correla- tion technique. *Limnol. Oceanogr.* 56, 86–96. doi: 10.4319/lo.2011.56.1.0086

Huthnance, J. M. (2010). "5.2. The Northeast Atlantic margins," in *Carbon and Nutrient Fluxes in Continental Margins: A Global Synthesis*, eds K. K. Liu, L. Atkinson, R. Quinones, and L. Talaue-Mcmanus (Berlin: Springer-Verlag), 215–234.

Kim, S. C., Friedrichs, C. T., Maa, J. P.-Y., and and Wright, L. D. (2000). Estimating bottom stress in tidal boundary layer from acoustic doppler velocimeter data. *J. Hydraul. Eng.* 126, 399–406. doi: 10.1061/(ASCE)0733-9429(2000)126:6(399)

Klitgaard, A. B., and Tendal, O. S. (2004). Distribution and species composition of mass occurrences of large-sized sponges in the northeast Atlantic. *Prog. Oceanogr.* 61, 57–98. doi: 10.1016/j.pocean.2004.06.002

Kutti, T., Bannister, R. J., and Fossa, J. H. (2013). Community structure and ecological function of deep-water sponge grounds in the Traenadypet MPA-Northern Norwegian continental shelf. *Cont. Shelf Res.* 69, 21–30. doi: 10.1016/j.csr.2013.09.011

Kutti, T., Bergstad, O. A., Fossa, J. H., and Helle, K. (2014). Cold-water coral mounds and sponge-beds as habitats for demersal fish on the Norwegian shelf. *Deep Sea Res. II Top. Stud. Oceanogr.* 99, 122–133. doi: 10.1016/j.dsr2.2013.07.021

Laberg, J. S., Vorren, T. O., Mienert, J., Bryn, P., and Lien, R. (2002). The Traenadjupet Slide: a large slope failure affecting the continental margin of Norway 4,000 years ago. *Geo-Mar. Lett.* 22, 19–24. doi: 10.1007/s00367-002-0092-z

Lindberg, B. (2004). *Cold-Water Coral Reefs on the Norwegian Shelf - Acoustic Signature, Geological, Geomorphological and Environmental Setting*. Ph.D., University of Tromsø.

Long, M. H., Berg, P., De Beer, D., and Zieman, J. C. (2013). *In situ* coral reef oxygen metabolism: an eddy correlation study. *PLoS ONE* 8:e58581. doi: 10.1371/journal.pone.0058581

Lorke, A., McGinnis, D. F., and Maeck, A. (2013). Eddy-correlation measurements of benthic fluxes under complex flow conditions: effects of coordinate transformations and averaging time scales. *Limnol. Oceanogr. Methods* 11, 425–437. doi: 10.4319/lom.2013.11.425

Lorrai, C., Mcginnis, D. F., Berg, P., Brand, A., and Wuest, A. (2010). Application of oxygen eddy correlation in aquatic systems. *J. Atmos. Ocean. Technol.* 27, 1533–1546. doi: 10.1175/2010JTECHO723.1

Maier, C., Hegeman, J., Weinbauer, M. G., and Gattuso, J. P. (2009). Calcification of the cold-water coral Lophelia pertusa under ambient and reduced pH. *Biogeosciences* 6, 1671–1680. doi: 10.5194/bg-6-1671-2009

Mcginnis, D. F., Berg, P., Brand, A., Lorrai, C., Edmonds, T. J., and Wuest, A. (2008). Measurements of eddy correlation oxygen fluxes in shallow freshwaters: towards routine applications and analysis. *Geophys. Res. Lett.* 35, L04403. doi: 10.1029/2007GL032747

Mienis, F., De Stigter, H. C., De Haas, H., and Van Weering, T. C. E. (2009). Near-bed particle deposition and resuspension in a cold-water coral mound area at the Southwest Rockall Trough margin, NE Atlantic. *Deep Sea Res. I Oceanogr. Res. Pap.* 56, 1026–1038. doi: 10.1016/j.dsr.2009.01.006

Miller, R. J., Hocevar, J., Stone, R. P., and Fedorov, D. V. (2012). Structure-forming corals and sponges and their use as fish habitat in bering sea submarine canyons. *PLoS ONE* 7:e33885. doi: 10.1371/journal.pone.0033885

Purser, A., and Thomsen, L. (2012). Monitoring strategies for drill cutting discharge in the vicinity of cold-water coral ecosystems. *Mar. Pollut. Bull.* 64, 2309–2316. doi: 10.1016/j.marpolbul.2012.08.003

Pusceddu, A., Bianchelli, S., Martin, J., Puig, P., Palanques, A., Masque, P., et al. (2014). Chronic and intensive bottom trawling impairs deep-sea biodiversity and ecosystem functioning. *Proc. Natl. Acad. Sci. U.S.A.* 111, 8861–8866. doi: 10.1073/pnas.1405454111

Reba, M. L., Link, T. E., Marks, D., and Pomeroy, J. (2009). An assessment of corrections for eddy covariance measured turbulent fluxes over snow in mountain environments. *Water Resour. Res.* 45, W00D38. doi: 10.1029/2008WR007045

Reimers, C. E., H. T. Özkan-Haller, P., Berg, A., Devol, K., and McCann-Grosvenor, and, R. D., Sanders (2012). Benthic oxygen consumption rates during hypoxic conditions on the Oregon continental shelf: evaluation of the eddy correlation method. *J. Geophys. Res.* 117, C02021. doi: 10.1029/2011jc007564

Ren, H., and Wu, Y. (2011). Turbulent boundary layers over smooth and rough forward-facing steps. *Phys. Fluids* 23, 045102. doi: 10.1063/1.3576911

Roberts, J. M., and Cairns, S. D. (2014). Cold-water corals in a changing ocean. *Curr. Opin. Environ. Sustain.* 7, 118–126. doi: 10.1016/j.cosust.2014.01.004

Roberts, J. M., Wheeler, A. J., and Freiwald, A. (2006). Reefs of the deep: the biology and geology of cold-water coral ecosystems. *Science* 312, 543–547. doi: 10.1126/science.1119861

Rovelli, L., Attard, K., Bryant, L. D., Flögel, S., Stahl, H., Roberts, J. M., et al. (2015). Benthic O_2 uptake of two cold-water coral communities estimated with the non-invasive eddy correlation technique. *Mar. Ecol. Prog. Ser.* 525, 97–104. doi: 10.3354/meps11211

Schluter, M., Sauter, E. J., Schafer, A., and Ritzrau, W. (2000). Spatial budget of organic carbon flux to the seafloor of the northern North Atlantic (60 degrees N-80 degrees N). *Global Biogeochem. Cycles* 14, 329–340. doi: 10.1029/1999GB900043

Slagstad, D., Tande, K. S., and Wassmann, P. (1999). Modelled carbon fluxes as validated by field data on the north Norwegian shelf during the productive period in 1994. *Sarsia* 84, 303–317.

Tjensvoll, I., Kutti, T., Fosså, J. H., and Bannister, R. J. (2013). Rapid respiratory responses of the deep-water sponge *Geodia barretti* exposed to suspended sediments. *Aquat. Biol.* 19, 65–73. doi: 10.3354/ab00522

Van Oevelen, D., Duineveld, G., Lavaleye, M., Mienis, F., Soetaert, K., and Heip, C. H. R. (2009). The cold-water coral community as a hot spot for carbon cycling on continental margins: a food-web analysis from Rockall Bank (northeast Atlantic). *Limnol. Oceanogr.* 54, 1829–1844. doi: 10.4319/lo.2009.54.6.1829

Wagner, H., Purser, A., Thomsen, L., Jesus, C. C., and Lundalv, T. (2011). Particulate organic matter fluxes and hydrodynamics at the Tisler cold-water coral reef. *J. Mar. Syst.* 85, 19–29. doi: 10.1016/j.jmarsys.2010.11.003

White, M., Wolff, G. A., Lundalv, T., Guihen, D., Kiriakoulakis, K., Lavaleye, M. S. S., et al. (2012). Cold-water coral ecosystem (Tisler Reef, Norwegian Shelf) may be a hotspot for carbon cycling. *Mar. Ecol. Prog. Ser.* 465, 11–23. doi: 10.3354/meps09888

Conflict of Interest Statement: The authors declare that the research was conducted in the absence of any commercial or financial relationships that could be construed as a potential conflict of interest.